

# The characterization of cake structure and rheology via pressureless slip casting

I. TSAO, R. A. HABER

*Department of Ceramic Science and Engineering, Rutgers University, PO Box 909, Piscataway, NJ 08855, USA*

For an aqueous alumina slip having an average particle size of  $0.5\ \mu\text{m}$ , the cake structure and rheology were investigated. Tetrasodium pyrophosphate (TSP) was chosen as a dispersant. Results showed that a partially flocculated slip (adding 0.28 wt% TSP based on solids) had higher viscosity but faster casting rate in comparison to a deflocculated slip (adding 0.42 wt% TSP). The resultant cake from the partially flocculated slip had an average green density of  $2.24\ \text{g cm}^{-3}$ , which was very close to the  $2.30\ \text{g cm}^{-3}$  for the cake cast from the deflocculated slip. However, the former had a more uniform pore-size distribution across the cake thickness than the latter. Cake rheology was characterized *in situ* using a parallel-plate rheometer. When the drying time (after casting) was less than 30 min, the cake from the partially flocculated slip resulted in higher elastic moduli and yield stresses compared to the deflocculated slip. However, at a drying time of 60 min, cakes grown from the flocculated slips exhibited lower elastic moduli and yield stresses. For all cakes studied, the critical elastic deformation before plastic flow was approximately equal to the average alumina powder diameter (i.e.  $\sim 0.5\ \mu\text{m}$ ). Finally, the rheological behaviour of alumina slip with larger particle size (i.e.  $\sim 1.2\ \mu\text{m}$ ) and broader size distribution was compared to that of the fine alumina. Results showed that these alumina cakes exhibited significantly greater plastic flow, in contrast to the  $0.5\ \mu\text{m}$  alumina cakes. This is believed to be an effect of the broader particle-size distribution.

## 1. Introduction

In the past decade, ceramists have been studying the casting behaviour of alumina slips. The research work has included different subjects such as particle packing and slurry rheology. Phelps *et al.* [1] have thoroughly discussed the slip-casting technology for clay and non-clay oxide systems. Smith and Haber [2] used the particle-packing theory to optimize the solids loading of aqueous alumina slips. Sacks *et al.* [3] characterized the dispersion and rheological behaviour of alumina powder in a non-aqueous solvent. All these efforts aimed at achieving a better solids dispersion and improved microstructure with high green density.

A dispersed suspension usually is desired for the slip-casting process to maximize compact density. However, Funk [4] has indicated that the use of partially flocculated slips can increase the casting rate. This is because the flocs provide larger pores for faster dewatering. More importantly, the partially flocculated slips have been shown to exhibit plasticity (attributed to the higher moisture content in these systems), which is conducive to better demoulding and cast finishing. Mould release is a very critical step during the casting process. Poor demoulding behaviour can result from the cake sticking at the mould interface. It ultimately affects the cake structure and leads to cracking. In successful removal of the cast

body from the mould, the rheological behaviour of the consolidated cake (i.e. the still-moist cake) plays an important role. These rheological properties can be correlated with the cake microstructure for optimal demoulding.

For slip casting of ceramics, much research has been done, especially in the areas of suspension rheology before casting and microstructure evaluation after sintering. However, until a short time ago, no study concerning the rheological behaviour of the cast cake had been available. Lange and co-workers [5, 6] studied the influence of interparticle forces on particle consolidation via pressure casting. They found that a coagulated microstructure was formed by adjusting the pH of the suspension (i.e. adding salt) and resulted in a weaker network structure than did the flocculated slip. In their subsequent investigation, the cake rheology was characterized using a uniaxial mechanical testing machine [7]. A constant strain of 2% was applied to the pressure-cast alumina particles for 0.2 s. The applied strain was then released and the resultant stress responses were recorded as a function of pH values representing different states of solids dispersion. In Fig. 1, a typical example indicates that the stress of a solid-like material never relaxes completely compared to that of materials exhibiting liquid-like or Newtonian behaviour. Consequently, a large residual

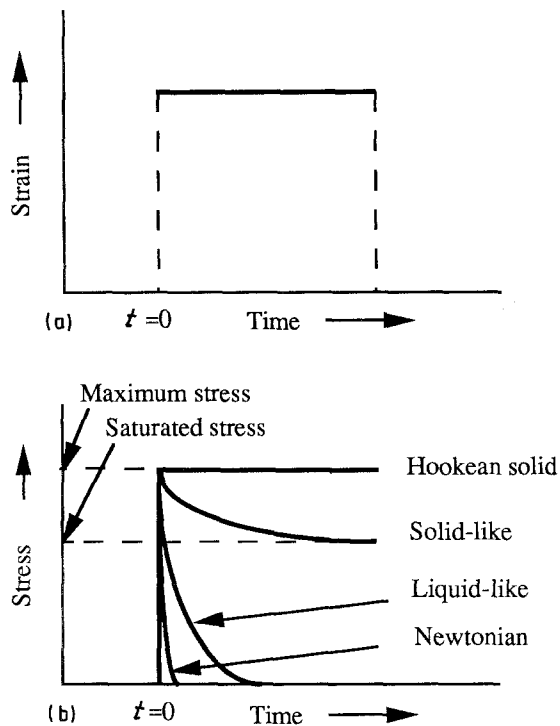


Figure 1 Stress relaxation of materials (after Velamakanni *et al.* [7]). (a) Imposed condition (b) response.

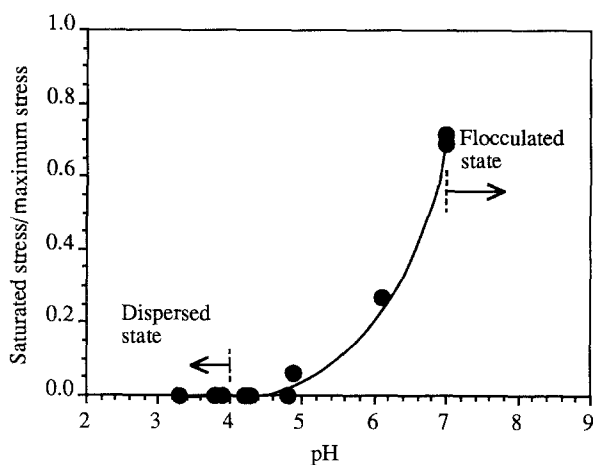


Figure 2 Stress relaxation versus pH for pressure-consolidated alumina at a strain of 2% (after Velamakanni *et al.* [7]).

stress is generated within a solid-like material, while the other two types have none or very little residual stress. Fig. 2 shows that, as a result, the ratio of the saturated stress (after relaxation) to the maximum stress (prior to relaxation) is nearly zero in a pH range of 3–5 (i.e. dispersed and coagulated states) in contrast to a value as high as 0.7 at pH 7 (i.e. flocculated state). Therefore, the flocculated cake could crack more than a dispersed or coagulated system after pressure release. One of the most important contributions of this work is that it represents the first application of cake rheology in the field of slip casting. Although the characterization was not conducted *in situ* (i.e. the microstructure might have been damaged slightly during sample removal), the results indicate that the rheological behaviour of the cast cake is very important and can be correlated with the microstructure. In

addition, the information concerning cake rheology helps to fill the knowledge gap between suspension rheology and final microstructure characterization for the entire casting process.

In this study, three different dispersion states of using a commercially available 0.5  $\mu\text{m}$  particle size alumina slips were pressureless cast to characterize the casting rate, cake structure and effect of drying time on cake rheology. Mercury porosimetry was employed to obtain the pore-size distribution from the cast bodies. The cake rheology was examined carefully in order to resolve the microstructural difference between the deflocculated, partially flocculated and flocculated systems. In addition, alumina powder with larger, more extended particle-size distribution was selected to study the effect of particle size on cake rheology. Rather than using uniaxial mechanical testing machine, a modified parallel plate rheometer was used to characterize cast cakes, using a sensitive transducer which was able to detect shear stress and shear strain relationship at a shear rate as low as  $10^{-6} \text{ s}^{-1}$ . All tests were conducted *in situ*, thus avoiding disturbing the cake, which could have altered its microstructure.

## 2. Experimental procedure

Aqueous slips of 76 wt% (or 42 vol%) A16-SG alumina were prepared with different dispersant concentrations. Tetrasodium pyrophosphate (TSPP) was dissolved in distilled and deionized water to be used as a dispersant. The ratio was fixed at 12 g TSPP/100 g water. All casts were made on 80 consistency plaster moulds. Deflocculation curves were attained using a Brookfield viscometer as seen in Fig. 3. Three slips, A, B and C, were selected at 0.25, 0.28 and 0.42 wt% TSPP additions, respectively, to represent the corresponding solids state of dispersion: flocculation, partial flocculation and deflocculation. In addition to A16-SG alumina, a dispersed Pechiney alumina slip (83 wt% or 55 vol% solids), was prepared at a TSPP concentration of 0.05 wt% to study the influence of particle size on cake rheology. All slips were ball milled for 1 h to breakup further large agglomerates. The particle-size distributions of both alumina systems were obtained using an X-ray sedigraph. As seen in Fig. 4, the Pechiney alumina exhibited a broader particle-size distribution and larger average diameter (1.35  $\mu\text{m}$ ) than the A16-SG alumina (0.55  $\mu\text{m}$ ).

To obtain the casting rate, cake thicknesses of the A16-SG alumina systems were measured as a function of drying time using a micrometer. Drying time is defined as the period of time the cake sets on the mould, once it has been cast from the slip. Afterwards, cakes grown from slips B and C for different times (1, 4 and 25 min) were partially sintered to 900  $^{\circ}\text{C}$  for 1/2 h at a ramp rate of 3  $^{\circ}\text{C min}^{-1}$ . This firing procedure was designed specifically to increase the cake strength for porosimetry measurements. For each cake cast at a different time, the top portion was sliced off (by grinding) as a measurement sample with a thickness of approximately 0.5 mm.

Finally, a modified parallel plate rheometer was used to study the cake rheology *in situ*. A pair of

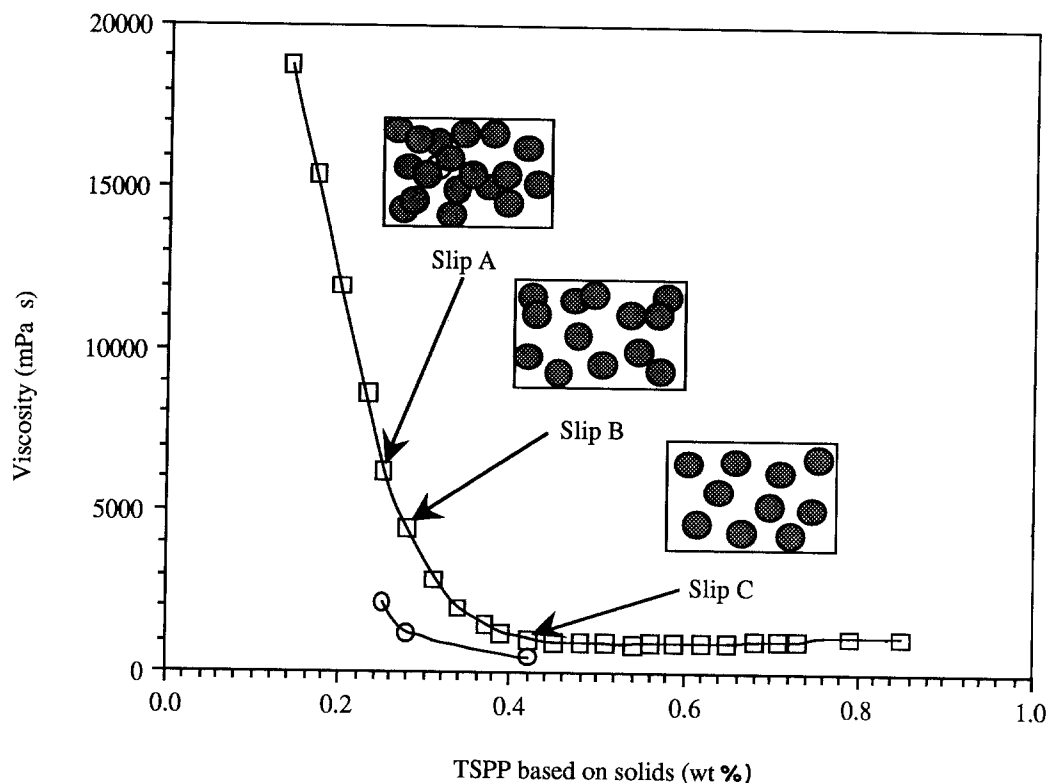


Figure 3 Deflocculation curve for A16-SG alumina slip (□) 3-blade mixer, (○) ball milling.

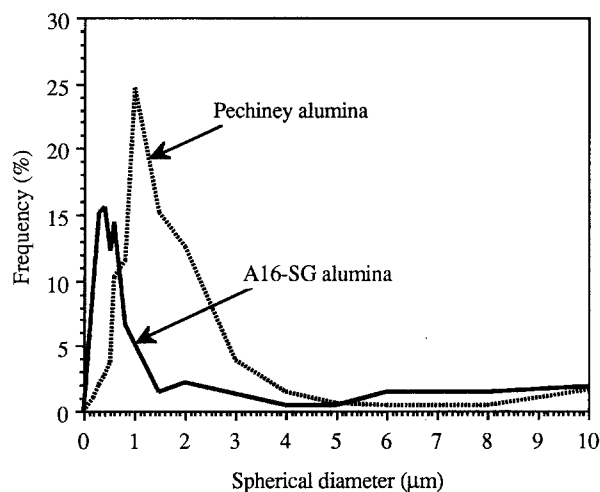


Figure 4 Frequency versus particle diameter for A16-SG and Pechiney alumina.

parallel plates was modified to be used as a measurement tool. The bottom plate, driven by a motor, was connected to an adapter on which a plaster mould was held within a ring (Fig. 5). Alumina slips were cast into an additional ring on the top of the plaster. The casting time was varied from 30–90 s, with the cake thickness precisely controlled by the gap between the two parallel plates (1.5 mm). The plaster was then saturated with moisture by injecting water from the bottom of the plaster cell using a syringe. This step eliminated the remaining drawing pressure from the mould. At drying times of 2, 10, 30, 60, 130 and 200 min, constant shear rate was applied immediately to characterize the cake structure *in situ*. The test parameter was a constant shear rate of  $10^{-4} \text{ s}^{-1}$  for 5 min.

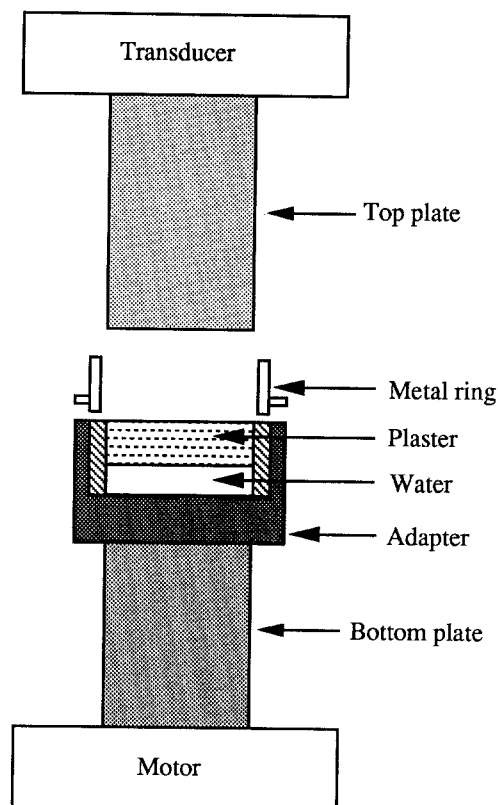


Figure 5 Schematic drawing of the parallel-plate tools.

### 3. Results and discussion

Suspension viscosities for slips A, B and C (after ball milling), in Fig. 3, were 2200, 1200 and 500 mPa s, respectively. Slip A was the most flocculated suspension; however, it was pourable and could be cast. When cake thicknesses were determined as a function

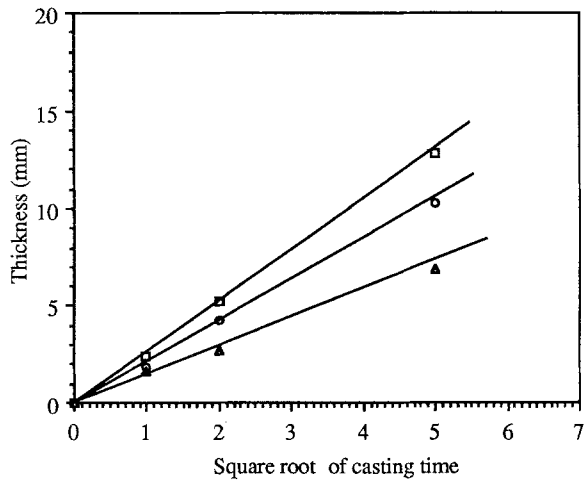


Figure 6 Cake thickness versus casting time for slips ( $\square$ ) A, ( $\circ$ ) B and ( $\Delta$ ) C,  $T = 25^\circ\text{C}$ .

of casting time for the three slips, the flocculated and partially flocculated slips showed higher casting rates, i.e. slip A > B > C (Fig. 6). This is because flocculation of slip increases the porosity and pore size of the cake, while the surface area remains the same.

To characterize cake structure, the pore-size distribution was obtained for both slip B (partially flocculated system) and slip C (deflocculated system) using a mercury porosimeter. Fig. 7 shows that the relative pore-size distribution, shown as the derivative of the cumulative curve, was very narrow for the cakes grown from slip B. The peaks of all three curves occur at essentially the same pore diameter of  $0.1\ \mu\text{m}$ . The superposition of the three curves indicates a uniform pore-size distribution as a function of cake thickness. The average green bulk density was calculated as  $2.24\ \text{g cm}^{-3}$ . Similarly, cakes grown from slip C also exhibit a very narrow pore-size distribution (Fig. 8) with an average green bulk density of  $2.30\ \text{g cm}^{-3}$ . However, the peak values of pore diameters for the 1 and 4 min cakes, were between  $0.08$  and  $0.09\ \mu\text{m}$ . These were clearly different from that of the 25 min cake (i.e.  $0.1\ \mu\text{m}$ ) which indicates non-uniform porosity across the cake. Hampton *et al.* [8] have shown

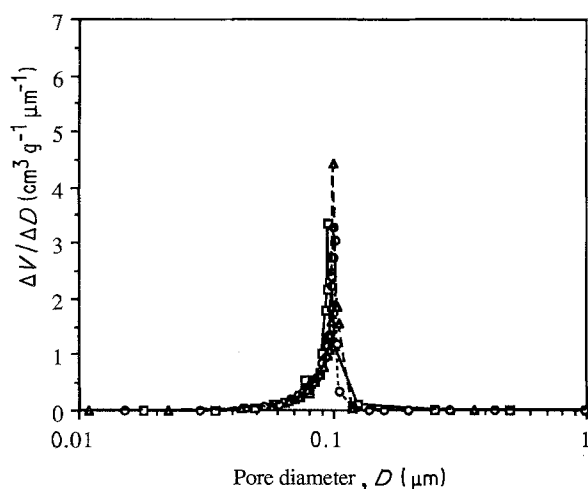


Figure 7 Relative pore-size distribution for cakes grown from slip B: ( $\square$ ) 1 min, ( $\circ$ ) 4 min, ( $\Delta$ ) 25 min.

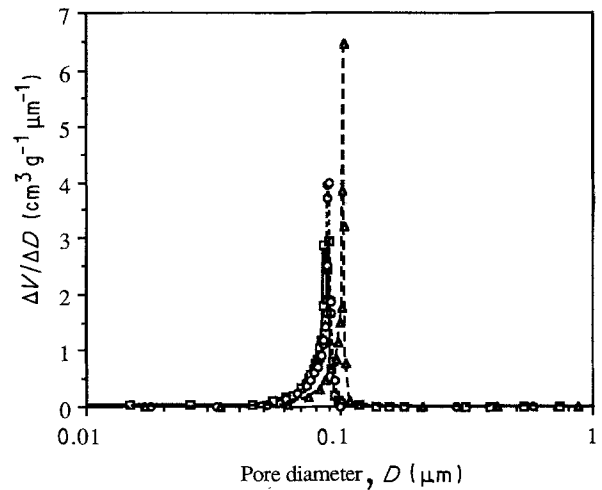


Figure 8 Relative pore-size distribution for cakes grown from slip C. For key, see Fig. 7.

that this can be attributed to the greater mobility of the dispersed particles, which initially are dragged together due to the suction pressure of the plaster. Afterwards, a dramatic reduction of the differential suction pressure results across the plaster and the initial cake due to the small pore size region (i.e. low permeability layer). Therefore, loose packed areas with larger pores are built up. For most non-plastic cakes, this non-uniform porosity can cause fracture during drying or a subsequent sintering stage. However, from the above discussion, it can be seen that the partially flocculated suspension, slip B, not only exhibits a faster casting rate, but also a smaller variation of pore size across the cake while still achieving an average green density comparable to the dispersed system.

Fig. 9 shows the shear stress-strain profile of slip A as a function of drying time. At 2 min, there is elastic behaviour as the shear stress gradually increases with increasing shear strain. However, a linear range is observed for the remaining three drying times, indicating a region of pure elastic behaviour. From the stress-strain curve, a yield point (i.e. proportion limit) can be determined. The yield stress is defined as an off-

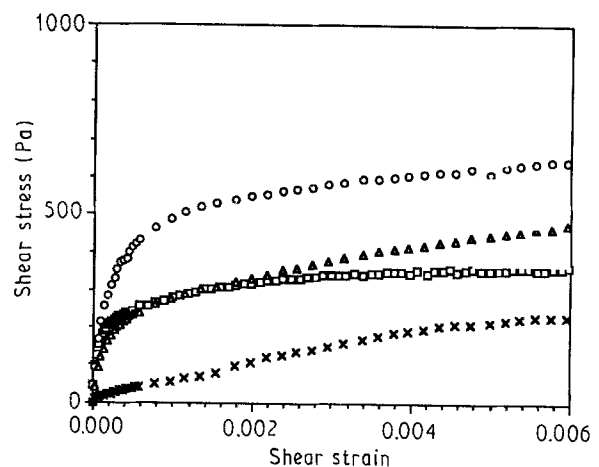


Figure 9 Shear stress versus shear strain for cast cake from slip A, at different drying times: ( $\times$ ) 2 min, ( $\Delta$ ) 10 min, ( $\circ$ ) 30 min, ( $\square$ ) 60 min.

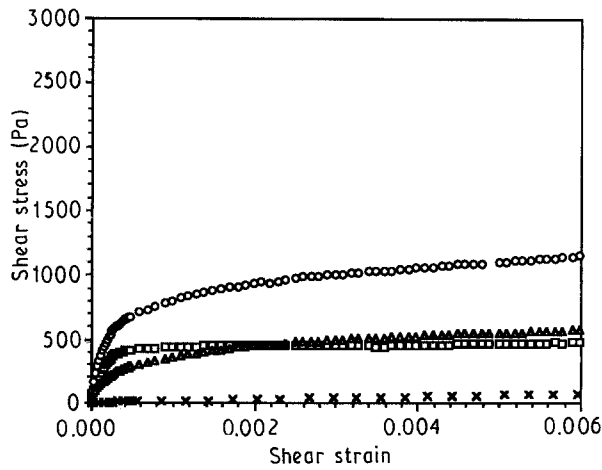


Figure 10 Shear stress versus shear strain for cast cake from slip B, at different drying times. For key, see Fig. 9.

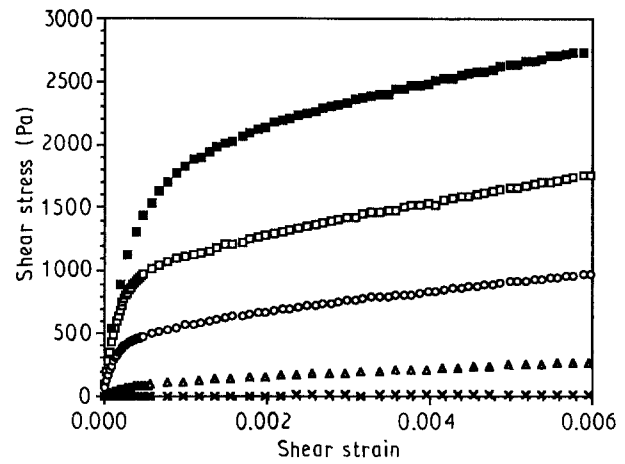


Figure 11 Shear stress versus shear strain for cast cake from slip C, at different drying times: (×) 2 min, (Δ) 10 min, (○) 30 min, (□) 60 min, (■) 200 min.

set stress for a 0.02 % strain. The elastic modulus, the slope over the linear region of each curve, also can be determined. The yield stress and elastic modulus usually are observed to increase with increasing drying time due to the increasing rigidity of the cake. However, the 60 min curve shows a much lower stress level compared to the 30 min curve. A short linear region is observed but is quickly followed by a nearly steady-state stress level instead of a plastic flow (i.e. gradually increasing stress). This suggests that the cake had already detached from the mould. This was also supported by visual observation, which showed the 60 min cake could be demoulded easily with little or no sticking. The same phenomenon was observed for slip B, as seen in Fig. 10. The only difference was that the stress levels of slip B were higher than those of slip A at the same drying time. This was due to better packing efficiency, which led to less residual moisture in the cake at each stage.

A different rheological behaviour was observed for slip C (the deflocculated slip). Fig. 11 shows that, except at 2 min, each curve exhibits a clear yield point and followed by plastic flow. However, the yield stress and elastic modulus increase with increasing drying time up to 200 min. These comparatively high stresses and moduli can be attributed to the superior packing state in slip C, where the cast cake retained the least moisture. In comparison with the behaviour of slips A and B, the continuous increase in yield stress for slip C indicates that the cake is still adhering firmly to the mould. This sticking phenomenon was verified by visual examination. In Fig. 12, the yield stresses of cakes resulting from different slips are plotted against the moisture content at different drying times. For slip C, the yield stress increases with decreasing the moisture content. On the contrary, for slips A and B, the yield stress decreases at lower moisture contents, which suggests that the cakes have demoulded. This decrease is because cast cake only experienced a partial deformation at the mould interface during measurement. Therefore, less torque was detected and it led to lower yield stress. For reference, the yield stresses

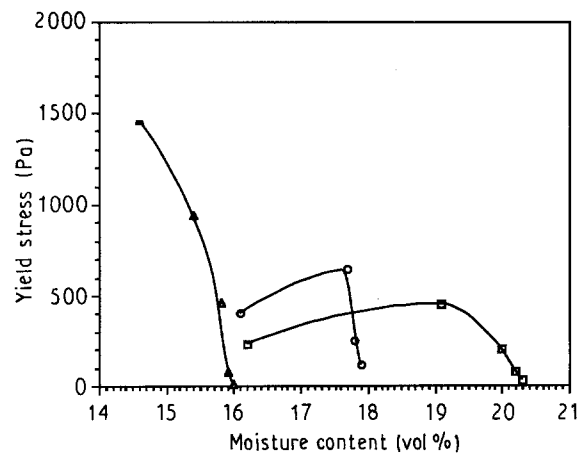


Figure 12 Yield stress versus moisture content for the cakes from slips (□) A, (○) B and (▲) C.

TABLE I Yield stresses and elastic moduli of the cast cakes

Slip	Drying time (min)	Yield stress, $\tau_y$ (Pa)	Elastic modulus $G$ (MPa)
A	2	28	0.7
	10	205	1.5
	30	455	4.1
	60	230	2.3
B	2	N/A	N/A
	10	250	1.9
	30	645	4.3
	60	402	2.2
C	2	N/A	N/A
	10	78	0.5
	30	460	2.9
	60	940	4.7
	200	1460	5.0

and elastic moduli of all cakes studied are summarized in Table I.

To study the effect of particle size on the cake rheology, the Pechiney, 1.2  $\mu\text{m}$ , alumina slip was dispersed with a viscosity of 73 mPa s. Fig. 13 shows the

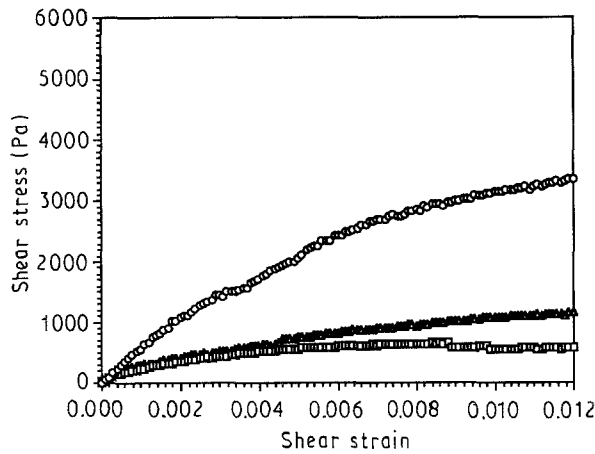


Figure 13 Shear stress versus shear strain for cast cake from Pechiney slip, at different drying times: ( $\Delta$ ) 10 min, ( $\circ$ ) 30 min, ( $\square$ ) 60 min.

stress-strain curves of the Pechiney system at drying times of 10, 30 and 60 min. In this figure, both shear stress and shear strain scales are enlarged in comparison with Figs 9–11. As can be seen, the cakes formed from the Pechiney slip exhibit a strong plastic flow type of stress-strain relationship. The elastic-plastic transition is very gradual, in contrast to the A16-SG system, making it very difficult to define the elastic regions and yield points for the three curves. This could be due to larger particle size and broader size distribution of the Pechiney alumina in comparison to the A16-SG alumina (Fig. 4). Under a shear force, the smaller particles would be more easily rearranged into the interstices of larger particles, leading to a smooth deformation such as a plastic flow. The actual travelling path between particles could be very short, resulting in a low energy barrier to be overcome. On the other hand, the A16-SG alumina has a narrow particle-size distribution, which makes it more difficult for particles to move over each other. Fig. 13 shows that, in the Pechiney system, the 60 min curve has a low stress level than those at 10 and 30 min. Similar to the previous discussion of slips A and B, this is an indication of cake detachment from the mould interface. This easy demoulding behaviour (supported by visual examination) may be due to the larger particle size, which could prevent the blockage of the plaster surface.

Finally, the critical elastic strain (i.e. off-drying limit) of each cake from the A16-SG alumina was determined from Figs 9–11. This information could be

very useful to understand the cake microstructure. By definition [1] for a laminar flow within two parallel plates, the elastic modulus,  $G$ , can be obtained from the shear stress,  $\tau$ , shear strain,  $\gamma$ , plot

$$\tau = G\gamma \quad (1)$$

The shear strain,  $\gamma$ , is defined as

$$\gamma = \frac{d}{h} \quad (2)$$

where  $d$  is the shear deformation and  $h$  is the gap between two parallel plates, i.e. the cake thickness. The maximum elastic deformation is simply the product of the critical strain,  $\gamma$ , and cake thickness,  $h$ . The critical elastic strains of each system in this study are listed in Table II. With this information, the maximum elastic deformation can be calculated using Equation 2. The resultant maximum displacement of all cakes was equal to 0.5 or 0.6  $\mu\text{m}$ . These values are essentially the same as the average diameter of A16-SG alumina (0.55  $\mu\text{m}$ ). In Fig. 14, a microscopic model is used to describe the movement of particles under a shear force. On the left, at the beginning, the shaded sphere intends to climb over the black sphere. In the middle, within the elastic region, the shaded sphere nearly moves over the black sphere. On the right, after the force release, the deformation is recovered due to the return of the shaded sphere to its original position. If this did not happen, unrecovered plastic flow would occur within the cake. Ideally, the elastic deformation

TABLE II Critical strain and maximum elastic deformation of the cast cakes

Slip	Drying time (min)	Critical strain, $\gamma$ ( $10^{-4}$ )	Max. elastic deformation, $d$ ( $\mu\text{m}$ )
A	2	2.4	0.4
	10	3.4	0.5
	30	3.1	0.5
	60	3.0	0.5
B	2	N/A	N/A
	10	3.3	0.5
	30	3.5	0.5
	60	3.8	0.6
C	2	N/A	N/A
	10	3.6	0.5
	30	3.6	0.5
	60	4.0	0.6
	200	4.7	0.7

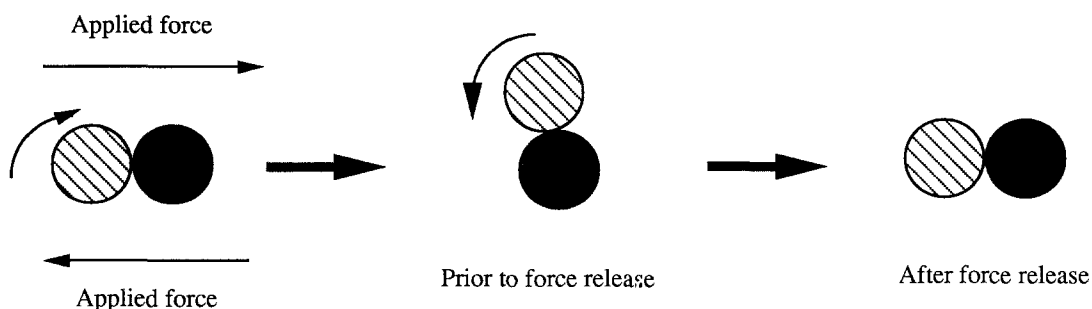


Figure 14 Elastic deformation between particles within cast cake.

should have the same order of magnitude as the sphere diameter. In fact, this has been demonstrated by the rheological characterization. Therefore, it can be seen that the cake rheology is very important and can be correlated with its microstructure during casting and demoulding.

#### 4. Conclusion

For the 0.5  $\mu\text{m}$  alumina system, the partially flocculated slip exhibited a faster casting rate and a more uniform porosity in comparison with the deflocculated slip. In addition, the partially flocculated system resulted in an average green cake density of 2.24  $\text{g cm}^{-3}$ , which was very close to the 2.30  $\text{g cm}^{-3}$  for the deflocculated slip. Of importance, the cake rheology was characterized *in situ* as a function of drying time using a modified parallel-plate rheometer. When the drying time was less than 30 min, the flocculated slips had higher yield stresses and elastic moduli compared to the deflocculated slip. This suggests that the cake formed from the partially flocculated system could be demoulded and subject to a greater strain. However, at a drying time of 60 min, the cake resulting from the flocculated slips showed lower yield stresses and elastic moduli. This could be attributed to the cake detachment at the mould interface. With the use of larger alumina particles, 1.2  $\mu\text{m}$ , all rheological curves exhibited plastic-flow behaviour and it was difficult to define the yield points. It was found that the cake of the coarser particle system could be demoulded easily at a drying time of 60 min. Finally, the maximum elastic deformation was calculated based on the cake rheology measurements. Results showed that the deformation was approximately equal to 0.5–0.6  $\mu\text{m}$ , i.e. the average diameter of a A16-SG alumina particle.

#### Acknowledgements

The authors thank Mr M. Lalwani for laboratory assistance and the Casting Technology Program of the Center for Ceramic Research at Rutgers University, for financial support.

#### References

1. G. W. PHELPS, S. G. MAGUIRE, J. KELLY and R. K. WOOD, in "Rheology and Rheometry of Clay Water Systems" (Cyprus Industrial Minerals Co., Sanderville, GA, 1983) pp. 1–110.
2. P. SMITH and R. A. HABER, *Ceram. Engng. Sci.* **12** (1991) 93.
3. M. D. SACKS, C. S. KHADILKAR, G. W. SCHEIFFELE, A. V. SHENOY, J. H. DOW and R. S. SHEU, in "Proceedings of the Ceramic Powder Science and Technology Conference: Synthesis, Processing, and Characterization," Boston, MA, August 1986, edited by G. L. Messing, K. S. Mazdiyasi, J. McCauley and R. A. Halser (American Ceramic Society, Inc., Westerville, OH, 1986) p. 495.
4. J. E. FUNK, in "Proceedings of a Special Conference of the 85th American Ceramic Society. Annual Meeting: Forming of Ceramics", Chicago IL, April 1983, edited by J.A. Mangels. (American Ceramic Society Inc., Westerville, OH, 1983) p. 76.
5. F. F. LANGE, B. V. VELAMAKANNI, J. C. CHANG and D. S. PEARSON, in "Proceedings of the 11th Risø International Symposium on Structural Ceramics - Processing, Microstructure and Properties", Denmark, September 1990, edited by J. J. Bentzen (Risø National Laboratory, Roskilde, Denmark, 1990) p. 57.
6. B. V. VELAMAKANNI, J. C. CHANG, F. F. LANGE and D. S. PEARSON, *Langmuir* **6** (1990) 1323.
7. B. V. VELAMAKANNI, F. F. LANGE and D. S. PEARSON, presented at the meeting of the American Ceramic Society, Anaheim, CA, November 1989.
8. J. HOLLY D. HAMPTON, S. B. SAVAGE and ROBIN A. L. DREW, *J. American Ceram. Soc.* **71** (1988) 1040.

*Received 4 February  
and accepted 20 November 1992*